Received: 27 January 2023 | Revised: 7 July 2023 | Accepted: 14 July 2023
DOI: 10.1111/exsy.13412

ORIGINAL ARTICLE

Expert Systems WILEY

A novel class of adaptive observers for dynamic nonlinear uncertain systems

Ahmed Alkhayyat[1] | Ali Mahdi Zalzala[2] | Asaad A. M. AL-Salih[3] | Anwar Ja'afar Mohamad Jawad[4] | Wameedh Riyadh Abdul-Adheem[5] | Jamshed Iqbal[6] | Ibraheem K. Ibraheem[7] | Waleed K. Ibrahim[8] | Mustafa Musa Jaber[9,10] | Asaad Shakir Hameed[11]

[1]College of Technical Engineering, The Islamic University, Najaf, Iraq
[2]Department of Electronics and Communication, College of Engineering, Uruk University, Baghdad, Iraq
[3]Department of Computer Engineering Techniques, Alnukhba University College, Baghdad, Iraq
[4]Department of Computer Techniques Engineering, Al-Rafidain University College, Baghdad, Iraq
[5]Department of Electrical Engineering, College of Engineering, University of Baghdad, Baghdad, Iraq
[6]Department of Computer Science and Technology, Faculty of Science and Engineering, University of Hull, Hull, UK
[7]Department of Computer Techniques Engineering, Dijlah University College, Baghdad, Iraq
[8]Department of Medical Instruments Engineering Techniques, Al-Farahidi University, Baghdad, Iraq
[9]Department of Medical Instruments Engineering Techniques, Dijlah University College, Baghdad, Iraq
[10]Department of Medical Instruments Engineering Techniques, Alturath University College, Baghdad, Iraq
[11]Department of Quality Assurance, Mazaya University College, Nasiriyah, Iraq

Correspondence
Ibraheem K. Ibraheem, Department of Computer Techniques Engineering, Dijlah University College, Baghdad 10001, Iraq.
Email: ibraheemki@coeng.uobaghdad.edu.iq

Abstract

Numerous techniques have been proposed in the literature to improve the performance of high-gain observers with noisy measurements. One such technique is the linear extended state observer, which is used to estimate the system's states and to account for the impact of internal uncertainties, undesirable nonlinearities, and external disturbances. This observer's primary purpose is to eliminate these disturbances from the input channel in real-time. This enables the observer to precisely track the system states while compensating for the various sources of uncertainty that can influence the system's behaviour. So, in this paper, a novel nonlinear higher-order extended state observer (NHOESO) is introduced to enhance the performance of high-gain observers under noisy measurement conditions. The NHOESO is designed to observe the system states and total disturbance while eliminating the latter in real time from the input channel. It is capable of handling disturbances of higher-order derivatives, including internal uncertainties, undesirable nonlinearities, and external disturbances. The paper also presents two innovative schemes for parametrizing the NHOESO parameters in the presence of measurement noise. These schemes are named time-varying bandwidth NHOESO (TVB-NHOESO) and online adaptive rule update NHOESO (OARU-NHOESO). Numerical simulations are conducted to validate the effectiveness of the proposed schemes, using a nonlinear uncertain system as a test case. The results demonstrate that the OARU technique outperforms the TVB technique in terms of its ability to sense the presence of noise components in the output and respond accordingly. However, it is noted that the OARU technique is slower than the TVB technique and requires more complex parameter tuning to adaptively account for the measurement noise.

KEYWORDS
adaptive observer, active disturbance rejection control; extended state observer; generalized disturbance; Lyapunov stability; nonlinear systems; system uncertainties

1 | INTRODUCTION

Many adaptive observers have been developed in the literature on automated control (Abdul-Adheem et al., 2020; Alain et al., 2019; Azar et al., 2020; Azar & Serrano, 2018; Djeddi et al., 2019; Kammogne et al., 2020). An active disturbance rejection control (ADRC) technique uses the extended state observer (ESO) for online uncertainty estimation. External disturbance inputs are treated as new state variables, and non-smooth, nonlinear error feedback control laws are applied to achieve state tracking by selecting proper parameters to observe all the system states and the exogenous disturbances. With ESO, a robust control system does not require an accurate model; it can cope with variations in parameter values and disturbances in the system. The reliability (robustness) of the control algorithm is the main emphasis of the robust control technique while designing controllers. The minimal standard that a control system must meet to be functional in a real-world setting is typically referred to as robustness. The ADRC controller offers the main advantage of requiring only a few tuning parameters, making real-world implementation easy. Yet, the absence of noise level in the control system is a need for ESO's capacity to quickly and precisely assess uncertainty and disruptions. Also, if there is measuring disturbance, the efficiency will be compromised or the device may potentially become unstable. Numerous studies have demonstrated that loud noise can increase errors, which raises the risk of accidents. This is very significant, especially when engaging in mental tasks that call for working memory, such as paying attention to multiple phenomena in complex systems. As a rule, higher tracking and disturbance rejection performance are generally associated with higher bandwidths for the observer and controller. If there are discrepancies between the actual system and the system model used to create the controller, the control system is robust. A measurement of the suppression of signals at y is called disturbance rejection. The design of the controller can be modified using PID Tuner to favour reference tracking or disturbance rejection depending on the needs of your application. Despite this, hardware factors such as sampling rates and noise limit the bandwidth. The observer parameters with large values can amplify measurement noise, which will degrade the performance of the ESO. The observer bandwidth should therefore be chosen to achieve an optimal balance between tracking performance and noise tolerance.

This research introduces the noisy environment observer and state reconstructor (NHOESO) to reconstruct the generalized disturbance and estimate system states in a noisy environment. Two parameterization schemes, namely time-varying bandwidth NHOESO (TVB-NHOESO) and online adaptive rule update NHOESO (OARU-NHOESO), enhance the NHOESO's performance. Practical measures like enclosures, barriers, and relocating noise sources are proposed to reduce noise in workplaces. Despite the accuracy and precision of measurements, inherent uncertainties from systematic and random errors should be considered.

1.1 | Problem statement

This problem can be mathematically stated by considering an uncertain nonlinear system of nth order with a relative degree ρ where $(\rho \le n)$,

$$\begin{cases} \xi^{(\rho)} = f\left(\xi, \ldots, \xi^{(\rho-1)}, \eta, w, t\right) + b(t)u \\ y = \xi + \mathcal{N} \\ \dot{\eta} = f_0\left(\eta, \xi, \ldots, \xi^{(\rho-1)}\right) \end{cases} \tag{1}$$

where $\mathcal{N} \in \mathbb{R}$ is the measurement noise, η is the internal dynamics, and w is the external disturbance. The system given in Equation (1) is not in the pure chain of integrators. Moreover, with noise, it is necessary to estimate the external states and generalized disturbances of Equation (1). The major objective of the external analysis is to identify the opportunities and threats in a field or business that will promote prosperity, expansion, and unpredictability. In addition, it directly threatens or damages actual or private possessions, and it irritates or disrupts a rational person with normal sensitivity. In this work, the estimated states ξ's are used for feedback, whilst cancelling the generalized disturbance from the nonlinear system of Equation (1) in the ADRC configuration.

1.2 | Paper contribution

The coefficients of the proposed observer are selected by two schemes to parametrize the proposed NHOESO have been given, namely TVB-NHOESO, and OARU-NHOESO. To the best of our knowledge, no study has been found in the literature that presents these kinds of parameter adaptations to the ESO to counteract the measurement noise.

1.3 | Paper organization

The remaining of the paper is organized as follows: the related works of the proposed model are discussed in Section 2; then the discussion about the proposed NHOESO is presented in Sections 3 and 4 provides a discussion about the proposed adaptive NHOESO; convergence analysis of the proposed observers is discussed in Section 5 and its sub-sections; the numerical simulation results of the proposed model is discussed in Section 6; finally, the conclusion of the proposed model is discussed in Section 7.

2 | RELATED WORKS

Noise presents significant challenges in various engineering applications. Efforts to attenuate the impact of noise usually involve the application of filters in system outputs; Filtered signals and actual system outputs typically differ in amplitude and phase, making it hard to overcome these differences. The scientific research community has reported several research works to address this problem. An enhanced ESO structure that augments another fictitious state variable to the conventional ESO was proposed by Madoński and Herman (2012) to form an integrated output signal. This resulted in increased performance in the observer. In another research work (Tamhane et al., 2018). Higher order sliding mode observer (HOSMO) with an integral surface was proposed, which provided attenuation of the estimation error to a small bound in the presence of measurement noise. In Liaquat et al. (2017), it was suggested that an n-link robot manipulator may have a prototype output feedback controller (OFBC). Utilizing a non-linear high-gain observation is accomplished. The measuring disturbance was greatly exacerbated in the situation of high workload viewers, leading to a greater steady-state inaccuracy. In Meyer et al. (2017), in a linear parameter variable (LPV) network, the assessment of the system parameters as well as the uncertain input is examined in the context of Gaussian white noise that influences both the state variables and the measuring formulas. An impartial observer with the smallest variance is used to make this assessment (as in Kalman filtering). In Yamada et al. (2019), reluctance torque is taken into account for the disturbance observer (DOB) and the reaction torque observer (RTOB). It is possible to design a control system with high torque and robust stability by changing the structure of the DOB when applying maximum torque per amplitude control (MTPAC). In Ali et al. (2019), two observers were designed and tested. For the output estimation, one extended high-gain observer was combined with another high-gain observer for the internal dynamic estimation. In contrast, the expanded high-gain observers assessed a pulse that the changes in the structure employed as a simulated output. In Sun et al. 2018), the frequency of a servo system was controlled by studying the mechanism and applying better techniques to remove disruption and noise. in Chen et al. (2019) an ESO was suggested to precisely predict the adhesive bond of railway cars while accounting for model uncertainties and parameter variations. The steady-state estimation error caused by the modelling deviation was eliminated with the help of an auxiliary compensation part based on the estimated modelling error information. Observer design via linear matrix inequalities is studied by Huang et al. (2020), Linares et al. (2022), and Mu et al. (2022). While Łakomy and Madonski (2021) applied cascade structure to design the ESO and finally Li and Xia (2020) proposed a scheme to adjust the gains of the linear ESO to counteract measurement noise. Pu et al. (2015) introduce a new class of adaptive extended state observers (AESOs) that extend the capabilities of ESOs to nonlinear disturbed systems. AESOs estimate states in nonlinear disturbed systems by combining an ESO with an adaptive mechanism. The AESOs transform the error dynamics into a canonical form and assign time-varying PD-eigenvalues. The paper presents two applications as examples and includes comparison simulations. Additionally, future work is emphasized for further investigation. Nonlinear adaptive observer design estimates states in uncertain dynamical systems by creating an observer system that adapts to uncertainties. The problem of adaptive state estimation for multivariable nonlinear systems in the presence of parameter uncertainty and bounded disturbances is addressed. A nonlinear adaptive observer with a time-varying gain matrix is used. Lyapunov arguments guarantee stability for state and parameter errors. This approach allows for perturbations without the need for the assumption of SPR to prove stability (Vargas & Hemerly, 2000). ESO, a kind of high-gain observers, are useful for regulating the outgoing return of unpredictable nonlinear networks. While utilizing nonlinear gain methods has the possibility of improving efficiency, the high-gain viewer is an effective and strong instrument for condition monitoring in unpredictable nonlinearities.

3 | THE PROPOSED NHOESO

Two key advances are introduced in this study to expand the idea of the linear extended state observer (LESO). A linear output feedback controller relying on ESOs is developed to address trajectory tracking concerns depending on a category of disturbed proportionally flattened machines. Firstly, incorporating a smooth nonlinear error function in the LESO, which satisfies the rule, 'small error, big gain' or 'big error, small gain' to compress the estimation error. Secondly, adding an extra augmented state to the proposed nonlinear ESO to estimate the generalized disturbance $\xi_{\rho+1}$ asymptotically with an estimation error $e_i(t), i \in \{1,2,..,\rho+1\}$. As the second derivative of the generalized disturbance $\xi_{\rho+1}$ increases in magnitude, the error escalates as well. These two improvements are instrumental in enabling the NHOESO to estimate uncertainties and disturbances with higher-order derivatives. This provides faster and more accurate estimations of the generalized disturbance $\xi_{\rho+1}$ and states $\xi_i, i \in \{1,2,...,\rho\}$. The proposed nonlinear error function also reduces the chattering phenomenon, which inherently exists in LESOs. The switching surface is surrounded by a boundary layer to decrease chattering in sliding-mode control, while continuous control is employed inside the boundary. It is examined how different control laws within the boundary layer affect chattering as well as error convergence in diverse systems. Moreover, the suggested NHOESO results in a little output response overshoot and a smooth control signal given. Given the nonlinear system of (1) and assuming $\xi_1 = y, \xi_2 = \dot{y}...., \xi_\rho = \xi^{(\rho-1)}$, yields,

$$\begin{cases} \dot{\xi}_i = \xi_{i+1}\, i \in \{1,2....,\rho-1\} \\ \dot{\xi}_\rho = f(\xi_1,\xi_2,...,\xi_\rho,w,t) + (b(t)-b_0)u + b_0 u \end{cases} \tag{2}$$

Augmenting the system with an additional state:

$$\xi_{\rho+1} = f + (b(t)-b_0)u = L \tag{3}$$

where $L = f + (b(t)-b_0)u$ includes the unknown uncertainties, internal dynamics exogenous, and disturbances and is referred to as a generalized disturbance. There are two approaches to choosing the coefficient value $b_0 \in \mathbb{R} \backslash \{0\}$:

1. The coefficient b_0 is an approximation of $b(t)$ in the plant of a range ± 50% (Han, 2009).
2. The coefficient b_0 is typically selected by the user directly as a design variable (Przybyła et al., 2012).

Start from (1) and augmenting the additional state $\xi_{\rho+1} = f + (b(t)-b_0)u = L$, $\xi_{\rho+2} = \dot{L}$, the system can be formulated as,

$$\begin{cases} \xi_i = \xi_{i+1}, i \in \{1,2,...,\rho-1\} \\ \dot{\xi}_\rho = \xi_{\rho+1} + b_0 u \\ \dot{\xi}_{\rho+1} = \xi_{\rho+2} \\ \dot{\xi}_{\rho+2} = \Delta_h \end{cases} \tag{4}$$

where $\Delta_h(t) = \ddot{L}$.

The proposed NHOESO is described as

$$\begin{cases} \dot{\hat{\xi}}_i = \hat{\xi}_{i+1} + \beta_i \mathscr{g}\left(y - \hat{\xi}_1\right), i \in \{1,2....,\rho-1\} \\ \dot{\hat{\xi}}_\rho = \hat{\xi}_{\rho+1} + \beta_\rho \mathscr{g}\left(y - \hat{\xi}_1\right) + b_0 u \\ \dot{\hat{\xi}}_{\rho+1} = \hat{\xi}_{\rho+2} + \beta_{\rho+1} \mathscr{g}\left(y - \hat{\xi}_1\right) \\ \dot{\hat{\xi}}_{\rho+2} = \beta_{\rho+2} \mathscr{g}\left(y - \hat{\xi}_1\right) \end{cases} \tag{5}$$

where β_is are observer gains to be tuned, $i = \{1,2,...,\rho+2\}$. Let $\beta_i = a_i {\omega_0}^i$, where a_i, $i \in \{1,2....,\rho+2\}$ is the design parameter associated with ${\omega_0}^i$, ω_0 is the bandwidth of NHOESO.

The mapping $\mathscr{g} : \mathbb{R} \to \mathbb{R}$ is selected as,

$$\mathscr{g}(e) = K_\alpha |e|^\alpha \mathrm{sign}(e) + K_\beta |e|^\beta e \tag{6}$$

where $K_\alpha, K_\beta, \alpha, \text{and}\, \beta$ are the positive design parameters, $e = y - \hat{\xi}_1$. The proposed nonlinear function given in Equation (6) can be written as:

$$\mathscr{g}(e) = \left(K_\alpha \frac{|e|^\alpha}{e} \mathrm{sign}(e) + K_\beta |e|^\beta\right) e \tag{7}$$

Since sign $(e) = e/|e|$, for $|e| \neq 0$, then

$$\mathscr{g}(e) = \begin{cases} 0 & e = 0 \\ k(e)e & e \neq 0 \end{cases} \tag{8}$$

The function $k : \mathbb{R}/\{0\} \to \mathbb{R}^+$ is defined as,

$$k(e) = K_\alpha |e|^{\alpha-1} + K_\beta |e|^\beta \tag{9}$$

4 | THE PROPOSED ADAPTIVE NHOESO

The basic principle of the proposed adaptive NHOESO is to dynamically change some or all the ESO's parameters in such a way that it confers the ESO more immunity against the measurement noise $\mathcal{N}$ while achieving the required estimation accuracy. The following two novel schemes demonstrate this key idea.

4.1 | Scheme 1. TVB

In this scenario, we adaptively determine the NHOESO bandwidth under the minimization of the estimation error even in the existence of the measurement noise. The observer in this scheme is called TVB-NHOESO. Consider the proposed NHOESO described by:

$$\begin{cases} \dot{\hat{\xi}}_1 = \hat{\xi}_2 + a_1\hat{\omega}_0 \mathcal{g}\left(y-\hat{\xi}_1\right) \\ \dot{\hat{\xi}}_2 = \hat{\xi}_3 + a_2\hat{\omega}_0{}^2 \mathcal{g}\left(y-\hat{\xi}_1\right) \\ \qquad \vdots \\ \dot{\hat{\xi}}_\rho = \hat{\xi}_{\rho+1} + b_0 u + a_\rho\hat{\omega}_0{}^\rho \mathcal{g}\left(y-\hat{\xi}_1\right) \\ \dot{\hat{\xi}}_{\rho+1} = \hat{\xi}_{\rho+2} + a_{\rho+1}\hat{\omega}_0{}^{\rho+1} \mathcal{g}\left(y-\hat{\xi}_1\right) \\ \dot{\hat{\xi}}_{\rho+2} = a_{\rho+2}\hat{\omega}_0{}^{\rho+2} \mathcal{g}\left(y-\hat{\xi}_1\right) \end{cases} \tag{10}$$

where a_i, and $i \in \{1,2,\ldots,\rho+2\}$ are associated design parameters, and $\hat{\omega}_0$ is the estimated bandwidth parameter. A novel approach to update this parameter $\hat{\omega}_0$ is given as

$$\hat{\omega}_0 = \omega_{0\max} e^{-\varrho(t-t_c)^2} \tag{11}$$

where t_c is the centre time, $\omega_{0\max}$ is the maximum allowable bandwidth, and ϱ is the adaptation parameter. Different values of $\hat{\omega}_0$ can be obtained with various values of ϱ as shown in Figure 1. This scheme guarantees that the $\omega_{0\max}$ can be selected in the design to introduce maximum bandwidth at certain times by sliding t_c over the time axis. The most data that can be sent through an internet connection in a specific amount of time are known as max bandwidth. Then, fibre internet is the fastest connection you can get, but it is also the hardest to find. Cable is also reliable and has speeds faster than DSL internet.

The proposed TVB scheme is shown in Figure 2. The bandwidth of the NHOESO varies per time, as can be seen from (11). The parameters of (11) are selected to ensure that the $\omega_{0\max}$ is provided at t_c where the fast and accurate response of the error dynamics is required. The amplifier's gain is reduced by negative feedback. Moreover, it lessens inconsistency, loudness, and distortion. Disturbance signals, that reflect undesired impulses, influence the outcome of the management system and increase technical glitches. The time interval during which the bandwidth $\hat{\omega}_0$ is at its highest value is inversely proportional to ϱ (see Figure 1).

4.2 | Scheme 2. OARU

In contrast to the previous scheme, changing all the parameters of NHOESO tends to increase the accuracy of the state estimation. State estimation is a crucial component of power system control centres' online security analysis function. Tools for state estimation are employed at each substation to process these inaccurate measurements, filter them, identify mistakes, eliminate corrupt data, and determine the best estimate for the state variables. This enhances the convergence characteristics and suppresses the measurement noise more efficiently. It is motivated by a particular and compelling issue, whether that issue results from pressing social requirements or challenging scientific issues. And it exhibits a strong synergy between several fields. Moreover, reacting in response to the presence of noise is more effective compared to the TVB technique, when it comes to figuring out the quality and speed of a network or internet connection, TVB is a crucial component. In essence, your internet will be speedier and more effective the larger the bandwidth. Which changes the bandwidth irrespective of whether the noise $\mathcal{N}$ exists or not. The OARU-NHOESO is mainly based on the proposed adaptive law described by,

$$\dot{\theta} = -\tau\theta + |e_1|^{\alpha_s} \tag{12}$$

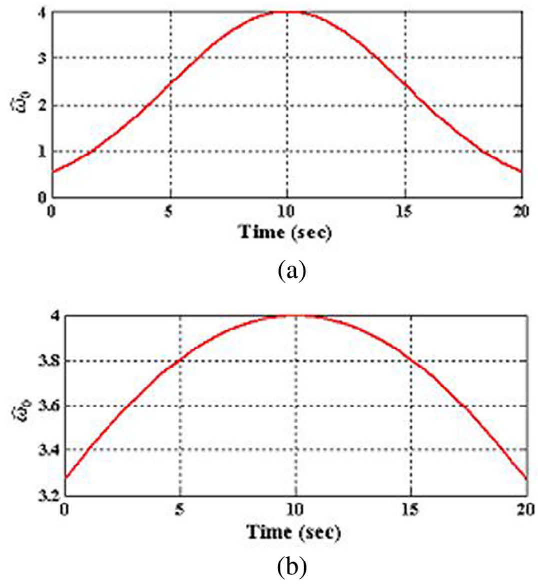

FIGURE 1 The nonlinear higher-order extended state observer (NHOESO) bandwidth $\widehat{\omega}_0$ versus time with $\omega_{0\max} = 4\frac{\text{rad}}{\text{sec}}$ and $t_c = 10\,\text{s}$ for, (a) $\varrho = 0.02$, (b) $\varrho = 0.002$.

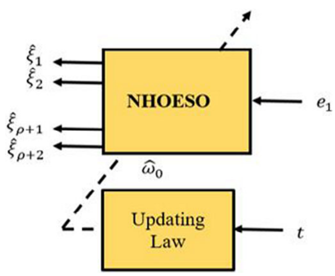

FIGURE 2 The structure of the time-varying bandwidth nonlinear higher-order extended state observer (TVB-NHOESO).

where τ is the exponential decay constant, θ is the adapted parameter and α_s is the noise-sensitive coefficient. The function $\propto(\cdot)$ is used to limit the value of the adaptation parameter, and is described as

$$\alpha(\theta) = \frac{1}{2}\tanh\left(\frac{\theta-\theta_c}{\kappa}\right) + \frac{1}{2} \tag{13}$$

where $\alpha : (-\infty,\infty) \to [0,1]$, is the limiting function, and θ_c and κ are function coefficients. The NHOESO parameters are defined as,

$$\Lambda = (\Lambda_u - \Lambda_l)\alpha(\theta) + \Lambda_l \tag{14}$$

where $\Lambda = (\beta_1,\beta_2,\beta_3,\beta_4,k_\alpha,k_\beta,\alpha,\beta)^T \in \mathbb{R}^8$ is the NHOESO parameter vector, Λ_l and Λ_u are the lower and upper bounds of the NHOESO parameters respectively. Figure 3 illustrates the structure of the OARU-NHOESO, which adapt the parameters of the NHOESO according to whether there is a noise in the output signal. You can forecast the noise form of an active device using noise characteristics. Nonetheless, everyone who builds a receiver should have a fundamental awareness of what noise circles on a Smith chart indicate. Noise parameters are typically left to LNA designers to consider. The detailed operation of this scheme is illustrated in Figure 4.

In the steady state, when the output is not contaminated with the measurement noise $\mathcal{N}$, the estimation error e_1 is almost zero. The Kalman filter's accurate error model can guarantee that the level of estimated accuracy is equivalent to the level of actual accuracy. The consistency between predicted accuracy and integrated accuracy will be impacted by inaccurate models. With unknown parameters, estimation is typically taken into account. If the true value is an estimate, then an error is merely the difference between the true value and forecast. Whereas, Decibels are used to measure noise level (dB). Decibel levels increase as noise levels do. To accommodate human hearing, decibels can be changed. Decibels A is the unit of measurement for noise level (dBA). At this point, the term $|e_1|^{\alpha_s}$ is also approximately zero. The adapted parameter θ will

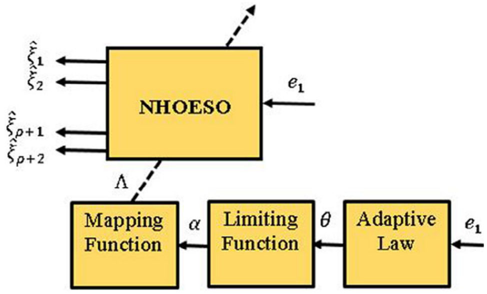

FIGURE 3 The structure of the online adaptive rule update nonlinear higher-order extended state observer (OARU-NHOESO).

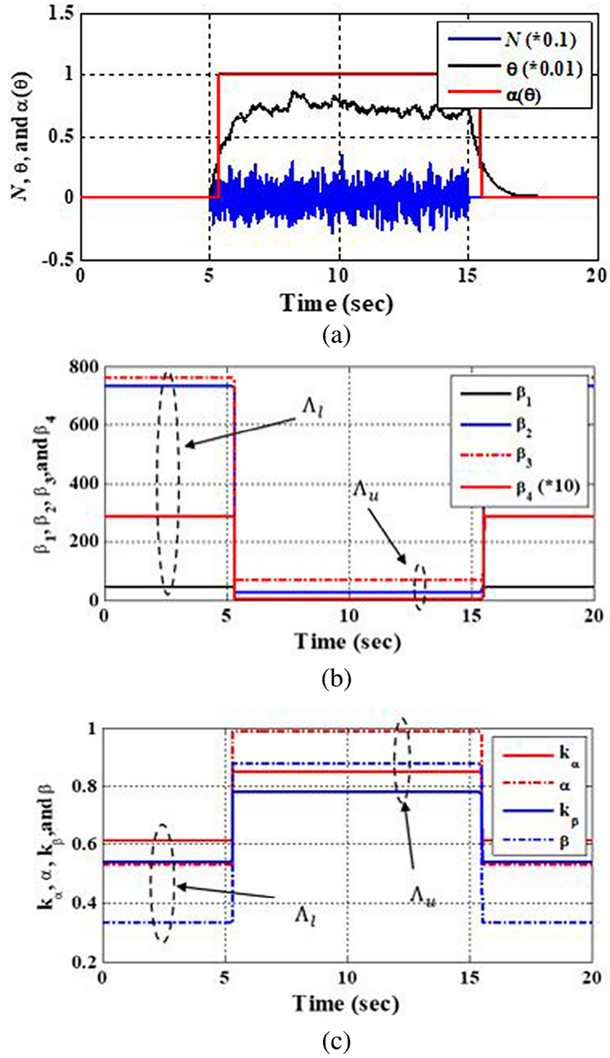

FIGURE 4 The time outputs of the online adaptive rule update (OARU) scheme with measurement noise, (a) $\mathcal{N}, \theta$, and $\alpha(\theta)$. (b) $\beta_1, \beta_2, \beta_3$, and β_4. (c) $k_\alpha, \alpha, k_\beta$, and β.

approach a value of zero after a certain period, depending on the value of τ, which leads $\alpha(\theta)$ to approach zero. In this case, Λ will take the lower set of parameters which corresponds to the noise-free case. On the other hand, adding a measurement noise will cause the estimation error e_1 at a steady state to have a non-negligible value and thus θ follows $|e_1|^{\alpha_s}$ and must have a value larger than θ_c to ensure $\alpha(\theta)$ approaches $+1$. Based on this value of $\alpha(\theta)$, Λ will approach Λ_u which is suitable in noisy environments.

Remark. The NHOESO has been tuned twice, once for obtaining the parameter set of a noise-free case Λ_l and the second tuning is to obtain the parameter set Λ_u which is concerned with measurement noise.

5 | CONVERGENCE ANALYSIS OF THE PROPOSED OBSERVERS

The following presumptions are necessary to demonstrate the consolidation of the NHOESO.

Assumption A2. The temporal component of the generalized disturbance has an upper constraint (i.e., at least $L \in C^1$ and $\sup_{t \in [0,\infty)} |L| = M < \infty$ where $\in \mathbb{R}$).

Assumption A3. L is a continuously differentiable function.

Assumption A4. There exists $M_h \in \mathbb{R}^+$ such that $sup_{t \in [0,\infty)} |\Delta_h(t)| = M_h$, where $\Delta_h(t) = \ddot{L}$.

Assumption A5. $V : \mathbb{R}^{\rho+2} \to \mathbb{R}^+$ and $W : \mathbb{R}^{\rho+2} \to \mathbb{R}^+$ are continuously differentiable functions with,

$$\lambda_1 \|\eta\|^2 \le V(\eta) \le \lambda_2 \|\eta\|^2, W(\eta) = \|\eta\|^2, \tag{15}$$

$$\sum_{i=1}^{\rho+1} \frac{\partial V(\eta)}{\eta_i} \left(\eta_{i+1} - a_i k \left(\frac{\eta_1}{\omega_0{}^{\rho}} \right) . \eta_1 \right) - \frac{\partial V(\eta)}{\partial y_{\rho+2}} a_{\rho+2} k \left(\frac{\eta_1}{\omega_0{}^{\rho}} \right) \eta_1 \le -W(\eta) \tag{16}$$

Theorem 1. **(NHOESO convergence):** *Given the system of* (1) *and NHOESO* (5), *it follows that*, *under* Assumptions A3, A4, and A5, *for any initial conditions*

$$\lim_{t \to \infty} \left| \xi_i(t) - \widehat{\xi}_i(t) \right| = O\left(\frac{1}{\omega_0{}^{\rho+3-i}} \right)$$

$$\lim_{\substack{t \to \infty \\ \omega_0 \to \infty}} \left| \xi_i(t) - \widehat{\xi}_i(t) \right| = 0$$

where ξ_i and $\widehat{\xi}_i$ symbolize the state of (6) and (7) respectively, with $i \in \{1, 2, \ldots, \rho+2\}$.

Proof. Let $e_i = \xi_i - \widehat{\xi}_i$, $i \in \{1, 2, \ldots, \rho+2\}$. Correspondingly, let

$$\eta_i = \omega_0{}^{\rho+1-i} e_i \left(\frac{t}{\omega_0} \right), i \in \{1, 2, \ldots, \rho+2\} \tag{17}$$

The evolution of the estimating error may therefore be described in terms of duration as,

$$\begin{cases} \dfrac{d\eta_1}{dt} = \eta_2 - a_1 k \left(\dfrac{\eta_1}{\omega_0{}^{\rho}} \right) \eta_1 \\ \dfrac{d\eta_2}{dt} = \eta_3 - a_2 k \left(\dfrac{\eta_1}{\omega_0{}^{\rho}} \right) \eta_1 \\ \quad \vdots \\ \dfrac{d\eta_\rho}{dt} = \eta_{\rho+1} - a_\rho k \left(\dfrac{\eta_1}{\omega_0{}^{\rho}} \right) \eta_1 \\ \dfrac{d\eta_{\rho+1}}{dt} = \eta_{\rho+2} - a_{\rho+1} k \left(\dfrac{\eta_1}{\omega_0{}^{\rho}} \right) \eta_1 \\ \dfrac{d\eta_{\rho+2}}{dt} = \dfrac{\Delta_h}{\omega_0{}^2} - a_{\rho+2} k \left(\dfrac{\eta_1}{\omega_0{}^{\rho}} \right) \eta_1 \end{cases} \tag{18}$$

■

Let the candidate Lyapunov functions $V, \mathbb{W} : \mathbb{R}^{\rho+2} \to \mathbb{R}^+$ denoted by $V(\eta) = < P\eta, \eta > = \eta^T P \eta$, with $\eta \in \mathbb{R}^{\rho+2}$ and P is a positive definite symmetric matrix. It is possible to tell if a system is stable or unstable using Lyapunov functions. This approach has the benefit of not needing us to be aware of the precise solution $x(t)$. Additionally, the stability of equilibrium points in non-rough systems can be investigated using this method. Examining the system's stability is beneficial. Consider (12) of Assumption A5 with $\lambda_1 = \lambda_{\min}(P)$ and $\lambda_2 = \lambda_{\max}(P)$, where $\lambda_{\min}(P)$ and $\lambda_{\max}(P)$ are the minimal and maximal eigenvalues of P, correspondingly. Finding $\dot{V}$ w.r.t t over η (over the solution (18)) is attained in the subsequent system,

$$\dot{V}(\eta)\big|_{\text{along (15)}} = \sum_{i=1}^{\rho+2} \frac{\partial V(\eta)}{\partial \eta_i} \dot{\eta}_i(t)$$

Then,

$$\dot{V}(\eta)\big|_{\text{along (15)}} = \sum_{i=1}^{\rho+1} \frac{\partial V(\eta)}{\eta_i}\left(\eta_{i+1}(t) - a_i k\left(\frac{\eta_1(t)}{\omega_0{}^{\rho}}\right).\eta_1(t)\right) - \frac{\partial V(\eta)}{\partial \eta_{\rho+2}} a_{\rho+2} k\left(\frac{\eta_1(t)}{\omega_0{}^{\rho}}\right).\eta_1(t) + \frac{\partial V(\eta)}{\partial \eta_{\rho+2}} \frac{\Delta_h}{\omega_0{}^2},$$

Consider (16) of Assumption A5, then, $\dot{V}(\eta)\big|_{\text{along (15)}} \le -W(\eta) + \frac{\partial V(\eta)}{\partial \eta_{\rho+2}} \frac{\Delta_h}{\omega_0{}^2}$.

As $V(\eta) \le \lambda_{\max}(P)\|\eta\|^2$ and $\left|\frac{\partial V(\eta)}{\partial \eta_{\rho+2}}\right| \le \left\|\frac{\partial V(\eta)}{\partial \eta}\right\|$, then $\left|\frac{\partial V}{\partial \eta_{\rho+2}}\right| \le 2\lambda_{\max}(P)\|\eta\|$. As $V(\eta) \le \lambda_{\max}(P)\|\eta\|^2 = \lambda_{\max}(P) W(\eta)$. Thus, $-W(\eta) \le -\frac{V(\eta)}{\lambda_{\max}(P)}$. Finally, because $\lambda_{\min}(P)\|\eta\|^2 \le V(\eta)$, this leads to $\|\eta\| \le \sqrt{\frac{V(\eta)}{\lambda_{\min}(P)}}$. Based on this and given Assumption A4, $\dot{V}(\eta)$ becomes,

$\dot{V}(\eta) \le -\frac{V(\eta)}{\lambda_{\max}(P)} + \frac{M_h}{\omega_0{}^2} 2\lambda_{\max}(P) \frac{\sqrt{V(\eta)}}{\sqrt{\lambda_{\min}(P)}}$. Since $\frac{d}{dt}\sqrt{V(\eta)} = \frac{1}{2}\frac{1}{\sqrt{V(\eta)}}\dot{V}(\eta)$, then,

$$\frac{d}{dt}\sqrt{V(\eta)} \le \frac{1}{2}\frac{1}{\sqrt{V(\eta)}}\left(-\frac{V(\eta)}{\lambda_{\max}(P)} + \frac{M_h}{\omega_0{}^2} 2\lambda_{\max}(P) \frac{\sqrt{V(\eta)}}{\sqrt{\lambda_{\min}(\eta)}}\right)$$

which gives

$$\frac{d}{dt}\sqrt{V(\eta)} \le -\frac{\sqrt{V(\eta)}}{2\lambda_{\max}(P)} + \frac{M_h}{\omega_0{}^2}\frac{\lambda_{\max}(P)}{\sqrt{\lambda_{\min}(P)}}. \tag{19}$$

Given that (19) is an ordinary first ODE, it can be solved as

$$\sqrt{V(\eta)} \le \frac{2M_h \lambda^2{}_{\max}(P)}{\omega_0{}^2 \sqrt{\lambda_{\min}(P)}}\left(1 - e^{-\frac{t}{2\lambda_{\max}(P)}}\right) + \sqrt{V(\eta(0))}\, e^{-\frac{t}{2\lambda_{\max}(P)}}$$

From Assumption A5, we have $\lambda_{\min}(P)\|\eta\|^2 \le V(\eta)$. This leads to $\|\eta\| \le \sqrt{\frac{V(\eta)}{\lambda_{\min}(P)}}$. Then,

$$\|\eta\| \le \sqrt{\frac{1}{\lambda_{\min}(P)}}\left(\frac{2M_h \lambda^2{}_{\max}(P)}{\omega_0{}^2 \sqrt{\lambda_{\min}(P)}}\left(1 - e^{-\frac{t}{2\lambda_{\max}(P)}}\right) + \sqrt{V(\eta(0))}\, e^{-\frac{t}{2\lambda_{\max}(P)}}\right)$$

which gives

$$\|\eta\| \le \frac{2M_h \lambda^2{}_{\max}(P)}{\omega_0{}^2 \lambda_{\min}(P)}\left(1 - e^{-\frac{t}{2\lambda_{\max}(P)}}\right) + \sqrt{\frac{V(\eta(0))}{\lambda_{\min}(P)}}\, e^{-\frac{t}{2\lambda_{\max}(P)}} \tag{20}$$

It results from (17) that,

$$\left|\xi_i - \hat{\xi}_i\right| \le \frac{1}{\omega_0{}^{\rho+1-i}}\|\eta(\omega_0 t)\|.$$

It follows from (19) that,

$$\left|\xi_i - \hat{\xi}_i\right| \le \frac{1}{\omega_0{}^{\rho+1-i}}\left(\frac{2M_h \lambda^2{}_{\max}(P)}{\omega_0{}^2 \lambda_{\min}(P)}\left(1 - e^{-\frac{\omega_0 t}{2\lambda_{\max}(P)}}\right) + \sqrt{\frac{V(\eta(0))}{\lambda_{\min}(P)}}\, e^{-\frac{\omega_0 t}{2\lambda_{\max}(P)}}\right)$$

Finally,

$$\lim_{t\to\infty}\left|\xi_i-\hat{\xi}_i\right|=\frac{1}{\omega_0{}^{\rho+3-i}}\frac{2M_h\lambda^2{}_{\max}(P)}{\lambda_{\min}(P)}=O\left(\frac{1}{\omega_0{}^{\rho+3-i}}\right) \tag{21}$$

and

$$\lim_{\substack{t\to\infty\\ \omega_0\to\infty}}\left|\xi_i-\hat{\xi}_i\right|=0.$$

5.1 | Justification for adding augmented state

This paragraph explains the rationale for including one further region in the proposed NHOESO. The analysis of the steady-state estimation error $e_i(t), i\in\{1,2,..,\rho+1\}$ of the LESO can be originated in (Abdul-Adheem et al., 2021),

$$\lim_{t\to\infty}\left|\xi_i-\hat{\xi}_i\right|=\frac{1}{\omega_0{}^{\rho+2-i}}\frac{2M\lambda^2{}_{\max}(P)}{\lambda_{\min}(P)} \tag{22}$$

while that of the NHOESO is found in Theorem 1,

$$\lim_{t\to\infty}\left|\xi_i-\hat{\xi}_i\right|=\frac{1}{\omega_0{}^{\rho+3-i}}\frac{2M_h\lambda^2{}_{\max}(P)}{\lambda_{\min}(P)} \tag{23}$$

These results illustrate that the steady-state estimation error $\lim_{t\to\infty}\left|\xi_i-\hat{\xi}_i\right|$ of the NHOESO is more sensitive to the increase in the bandwidth ω_0 than that of the LESO. If the true value is an estimate, then an error is merely the difference between the true value and forecast. Whereas, decibels are used to measure noise level (dB). Decibel levels increase as noise levels do. Everyone who builds a receiver should have a fundamental awareness of what noise circles on a Smith chart indicate. Noise parameters are typically left to LNA designers to consider. This is a result of the denominator being ω_0. Furthermore, the steady-state estimate inaccuracies are equivalent to M for the LESO as shown in (22) and to M_{h} for the NHOESO as shown in (23), where M_{h} and M are the limit limits of the secondly as well as first harmonics of the universal disturbances $(+1)$ correspondingly (see Assumptions A2 and A4).

Let us assume a generalized disturbance $\xi_{\rho+1}$, which is a linear function in time, that is, $L(t)=at$, where a is a constant. Then $\Delta=\dot{L}=a$ and $\Delta_h=\ddot{L}=0$, based on this, the upper bound M, is a non-zero constant, while M_{h} is zero. In this case, for a specific low value of ω_0, the steady-state estimation error of the NHOESO in (23) will be zero, while that of the LESO given in (22) has a non-negligible value. Therefore, the NHOESO is more suitable than the LESO to give an estimation of the generalized disturbance $\xi_{\rho+1}$ of linear type. Moreover, a generalized disturbance $\xi_{\rho+1}$ with a higher-order derivative will worsen the steady-state estimation error for the LESO, because if the generalized disturbance $\xi_{\rho+1}$ is expressed as $L(t)=at^2$, then, the upper bound $M\to\infty$, as $t\to\infty$. The steady-state estimation error of the LESO will escape to infinity, that is, $\lim_{t\to\infty}\left|\xi_i-\hat{\xi}_i\right|\to\infty$, and thus, LESO will diverge. However, M_{h} will have a constant value $(2a)$. Hence, with a sufficiently broad NHOESO spectrum ω_0, the NHOESO will have a minimal steady-state estimate error.

The next instance will investigate the NHOESO's single flaw: the amount of time needed for the predicted generalized disruption to subside to its real magnitude $\hat{\xi}_3$. When a relative degree is equal to $\rho=2$, the LESO is stated as

$$\begin{cases}\dot{\hat{\xi}}_1=\hat{\xi}_2+\beta_1\left(y-\hat{\xi}_1\right),\\ \dot{\hat{\xi}}_2=\hat{\xi}_3+\beta_2\left(y-\hat{\xi}_1\right)+b_0u,\\ \dot{\hat{\xi}}_3=\beta_3\left(y-\hat{\xi}_1\right).\end{cases} \tag{24}$$

and the dynamics of the NHOESO given in (5) with $g\left(y-\hat{\xi}_1\right)=y-\hat{\xi}_1$ is expressed as

$$\begin{cases}\dot{\hat{\xi}}_1=\hat{\xi}_2+\beta_1\left(y-\hat{\xi}_1\right),\\ \dot{\hat{\xi}}_2=\hat{\xi}_3+\beta_2\left(y-\hat{\xi}_1\right)+b_0u,\\ \dot{\hat{\xi}}_3=\hat{\xi}_4+\beta_3\left(y-\hat{\xi}_1\right),\\ \dot{\hat{\xi}}_4=\beta_4(y-\xi_1).\end{cases} \tag{25}$$

Given that $\hat{\xi}_4 = \int \beta_4 (y - \xi_1)\, dt$, then (23) can be expressed as,

$$\begin{cases} \dot{\hat{\xi}}_1 = \hat{\xi}_2 + \beta_1 \left(y - \hat{\xi}_1 \right), \\ \dot{\hat{\xi}}_2 = \hat{\xi}_3 + \beta_2 \left(y - \hat{\xi}_1 \right) + b_0 u, \\ \dot{\hat{\xi}}_3 = \beta_4 \int_0^t \left(y - \hat{\xi}_1 \right) dt + \beta_3 \left(y - \hat{\xi}_1 \right). \end{cases} \tag{26}$$

From (22) it is evident that the predicted generalized disruption $\hat{\xi}_3$ is a function of the error $e_1 = y - \hat{\xi}_1$ and will alter in line with the mistake. The price will settle at its true value ξ_3 whenever the estimation error $y - \hat{\xi}_1$ becomes zero. While in the NHOESO (26), furthermore, given the integration term $\beta_4 \int_0^t \left(y - \hat{\xi}_1 \right) dt$, a generalized disturbance estimates $\hat{\xi}_3$ of the NHOESO a while to achieve its true worth. ξ_3, which needs the subsequent condition:

$$\beta_4 \int_0^t \left(y - \hat{\xi}_1 \right) dt + \beta_3 \left(y - \hat{\xi}_1 \right) = 0 \tag{27}$$

Letting $e_1 = y - \hat{\xi}_1$. Then (27) can be expressed as

$$\beta_4 \int_0^t e_1\, dt + \beta_3 e_1 = 0, \tag{28}$$

Taking the derivative of (28) w.r.t t, we get

$$\dot{e}_1 = -\frac{\beta_4}{\beta_3} e_1 \tag{29}$$

Solving (27) w.r.t t, yields

$$e_1(t) = e_1(0) \exp\left(-\frac{\beta_4}{\beta_3} t \right)$$

Therefore, the condition (27) will be satisfied at $t \to \infty$ (i.e., $t = -\frac{\beta_3}{\beta_4} \ln\left(\frac{e_1(t)}{e_1(0)} \right)$ when $e_1(t)$ has a very small value), or as the ratio $\frac{\beta_4}{\beta_3}$ is large enough where $e_1(t) = e_1(0) \exp\left(-\frac{\beta_4}{\beta_3} t \right)$ will decay faster to zero.

5.2 | Mismatched disturbances

The ESO expects that the plant is stated in the usual form to meet the matching requirement (Chen & Xu, 2016; Xue & Huang, 2014). It can thus only be used to model systems that can be explicitly represented in the normalized form or by altering variables. It can be difficult to apply this transition in a structure with no motion. The selected control action maintains the system's output variables at zero. Zero dynamics refers to the internal dynamics of the system caused by an input that keeps the output permanently at zero. The system is said to as being in the minimum phase if the zero dynamics are (globally) asymptotically stable. The system must be stable for tiny changes in the system's input, starting circumstances, and parameters that do not result in significant changes in the system's output. Reason: A system is only considered stable if it is both BIBO stable and asymptotic stable. Moreover, certain nonlinear systems exhibit disruptions in a separate control input port, so these devices are unable to meet the matched requirement. When the nonlinear feature of the system quickly changes as a result of some modest changes to legitimate factors, such as time, nonlinear processes present one of the greatest obstacles and are difficult to control. The solution can become bifurcated as a result of nonlinearity. As a result, ADRC is no longer under the control of this discordant disruption as well as it once could. For example, the accompanying modelling technique, which has a lower rectangular shape and unmatched perturbation, falls into the category of indeterminate dynamic equations (Ding & Zhu, 2021; Du et al., 2012; Guo & Wu, 2017; Yang & Ding, 2017; Zhu, 2018).

$$\begin{cases} \xi_i = a_i \xi_{i+1} + \phi_i(\xi_1, \dots, \xi_i) + w_i, i \in \{1, 2, \dots, \rho - 1\} \\ \xi_\rho = \phi_\rho(\xi_1, \xi_2, \dots, \xi_\rho) + w_\rho + bu, \\ y = \xi_1. \end{cases} \tag{30}$$

where $\xi = (\xi_1(t), \xi_2(t), ..., \xi_\rho(t))^T \in \mathbb{R}^\rho$ is the system state, $y(t) \in \mathbb{R}$ is the measured output, $u(t) \in \mathbb{R}$ is the control input, $w_i(t) \in \mathbb{R}, i \in \{1, 2, ..., \rho\}$ is the unknown exogenous disturbance, and $b \in \mathbb{R}$ is the control coefficient. The function $\phi_i : \mathbb{R}^i \to \mathbb{R}, i \in \{1, 2, ..., \rho\}$.

Theorem 2. *A second-order nonlinear system in a lower triangular form with mismatched disturbances can be described as follows,*

$$\begin{cases} \dot{\xi}_1 = a_1\xi_2 + \phi_1(\xi_1) + w_1, \\ \dot{\xi}_2 = \phi_2(\xi_1, \xi_2) + w_2 + bu, \\ y = \xi_1. \end{cases} \tag{31}$$

where $\xi = (\xi_1(t), \xi_2(t))^T \in \mathbb{R}^2$ is the system state, $y(t) \in \mathbb{R}$ is the measured output, $u(t) \in \mathbb{R}$ is the control input, $w_i(t) \in \mathbb{R}, i \in \{1, 2\}$ is the unknown exogenous disturbance, and $b \in \mathbb{R}$ is the control coefficient. The function $\phi_i : \mathbb{R}^i \to \mathbb{R}, i \in \{1, 2\}$. If the function ϕ_1 and the exogenous disturbance w_1 are differentiable w.r.t t, the system (31) can be transformed into the following form,

$$\begin{cases} \dot{\tilde{\xi}}_1 = \tilde{\xi}_2, \\ \dot{\tilde{\xi}}_2 = f(\tilde{\xi}_1, \tilde{\xi}_2, w_1, \dot{w}_1, w_2) + \widehat{b}u, \\ y = \tilde{\xi}_1. \end{cases} \tag{32}$$

where $f(\tilde{\xi}_1, \tilde{\xi}_2, w_1, \dot{w}_1, w_2) = a_1\phi_2\left(\tilde{\xi}_1, \frac{\tilde{\xi}_2 - \phi_1(\tilde{\xi}_1) - w_1}{a_1}\right) + \frac{\partial\phi_1(\tilde{\xi}_1)}{\partial\tilde{\xi}_1}\tilde{\xi}_2 + a_1w_2 + \dot{w}_1$

and $\widehat{b} = a_1b$.

Proof of Theorem 2. Let $\tilde{\xi}_1 = \xi_1$, and $\tilde{\xi}_2 = \dot{\xi}_1$.Then,

$$\dot{\tilde{\xi}}_2 = a_1\dot{\xi}_2 + \frac{\partial\phi_1(\xi_1)}{\partial\xi_1}\dot{\xi}_1 + \dot{w}_1 \tag{33}$$

■

By substituting (29) in (31) we get

$$\dot{\tilde{\xi}}_2 = a_1\phi_2(\tilde{\xi}_1, \xi_2) + \frac{\partial\phi_1(\tilde{\xi}_1)}{\partial\tilde{\xi}_1}\tilde{\xi}_2 + a_1w_2 + \dot{w}_1 + a_1bu. \tag{34}$$

Since $\xi_2 = \frac{\tilde{\xi}_2 - \phi_1(\tilde{\xi}_1) - w_1}{a_1}$. Then, (34) can be expressed as,

$$\dot{\tilde{\xi}}_2 = a_1\phi_2\left(\tilde{\xi}_1, \frac{\tilde{\xi}_2 - \phi_1(\tilde{\xi}_1) - w_1}{a_1}\right) + \frac{\partial\phi_1(\tilde{\xi}_1)}{\partial\tilde{\xi}_1}\tilde{\xi}_2 + a_1w_2 + \dot{w}_1 + a_1bu$$

Finally, system (31) can be defined as,

$$\begin{cases} \dot{\tilde{\xi}}_1 = \tilde{\xi}_2, \\ \dot{\tilde{\xi}}_2 = f(\tilde{\xi}_1, \tilde{\xi}_2, w_1, \dot{w}_1, w_2) + \widehat{b}u, \\ y = \tilde{\xi}_1. \end{cases}$$

where

$$f(\tilde{\xi}_1, \tilde{\xi}_2, w_1, \dot{w}_1, w_2) = a_1\phi_2\left(\tilde{\xi}_1, \frac{\tilde{\xi}_2 - \phi_1(\tilde{\xi}_1) - w_1}{a_1}\right) + \frac{\partial\phi_1(\tilde{\xi}_1)}{\partial\tilde{\xi}_1}\tilde{\xi}_2 + a_1w_2 + \dot{w}_1$$

$$\widehat{b} = a_1b.$$

Theorem 2 can be generalized easily for ρth order uncertain nonlinear systems in a lower triangular form with mismatched disturbance $w_i(t), i \in \{1, 2.., \rho\}$ as in Equation (30).

6 | RESULTS AND DISCUSSIONS

To solve a hypothetical uncertain nonlinear system, we employ various techniques to validate its effectiveness. The approach involves identifying the graph of each equation, expressing them in standard form, and manipulating the coefficients of one variable to establish relationships. By adding or subtracting the equations, we eliminate one variable and solve for the remaining one. This iterative process helps us find solutions for the system of nonlinear equations. Structures with the dynamics given as,

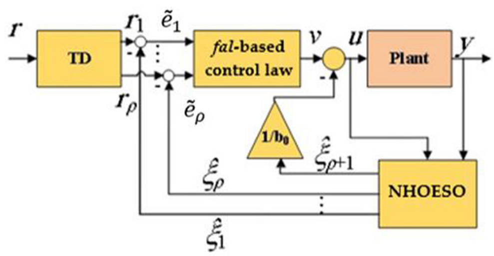

FIGURE 5 Structure of active disturbance rejection control (ADRC) with ρ relative degree.

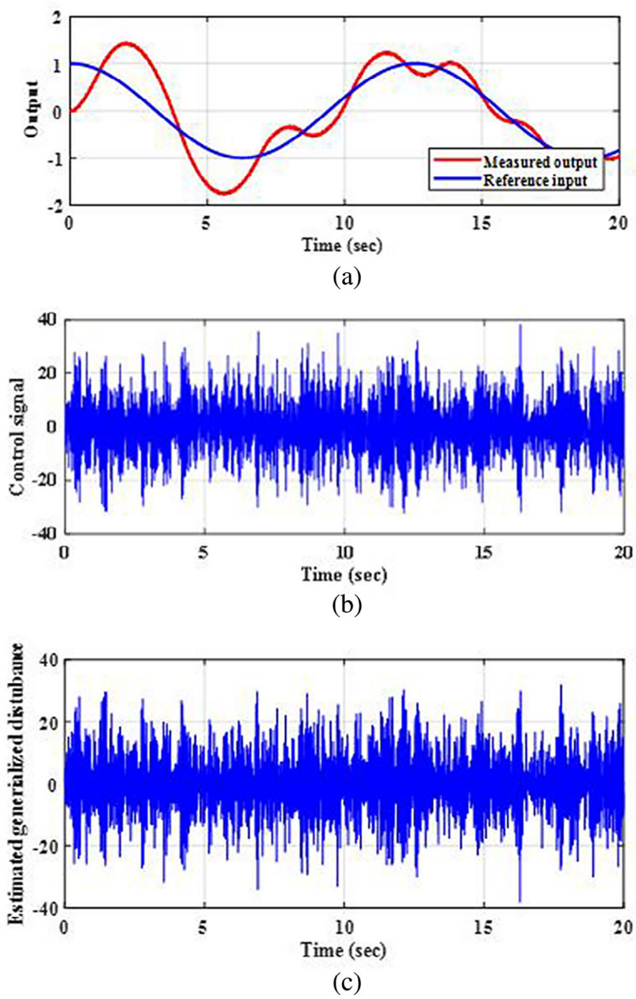

FIGURE 6 Response curves for Case Study 1, (a) tracking y of r, (b) control action u, (c) estimated generalized disturbance $\hat{\xi}_3$.

$$\begin{cases} \dot{\hat{\xi}}_1 = \hat{\xi}_2 \\ \dot{\hat{\xi}}_2 = f\left(\hat{\xi}_1, \hat{\xi}_2\right) + w(t) + (1 + a_3 \sin(t))u \\ y = x_1 \end{cases} \tag{35}$$

where $f\left(\hat{\xi}_1, \hat{\xi}_2\right) = a_1\hat{\xi}_1 + a_2 \sin\left(\hat{\xi}_2\right)$, with $a_1 = 0.2$, $a_2 = 0.1$, $a_3 = 0.1$, and the exogenous disturbance $w(t) = \exp(-t)\cos(t)$. A periodic signal is chosen to be $\cos(0.5t)$ applied at $t = 0$ s and inputted to the reference input $r(t)$.

A FAL-based control law utilizes fractional calculus principles to design control systems with non-integer dynamics. It involves applying fractional-order differential or integral operators to enhance control performance, adaptability, and robustness in various applications. This approach offers advantages such as improved accuracy and flexibility in modelling complex systems, making it applicable in fields like robotics, electrical systems, and biomedical engineering. The fal-based control law in this simulation is represented by,

$$u = \mathrm{fal}(\tilde{e}_1, \alpha_1, \delta_1) + \mathrm{fal}(\tilde{e}_2, \alpha_2, \delta_2) - \hat{\xi}_3 \tag{36}$$

The tracking error that drives the control law can be expressed as $(\tilde{e}_1, \tilde{e}_2)^T = (r_1, r_2)^T - \left(\hat{\xi}_1, \hat{\xi}_2\right)^T$. The desired transient profile vector $(r_1, r_2)^T$ is obtained using conventional TD given by:

$$\begin{cases} \dot{r}_1 = r_2, \\ \dot{r}_2 = -R\mathrm{sign}\left(r_1 - r + \frac{r_2|r_2|}{2R}\right) \end{cases} \tag{37}$$

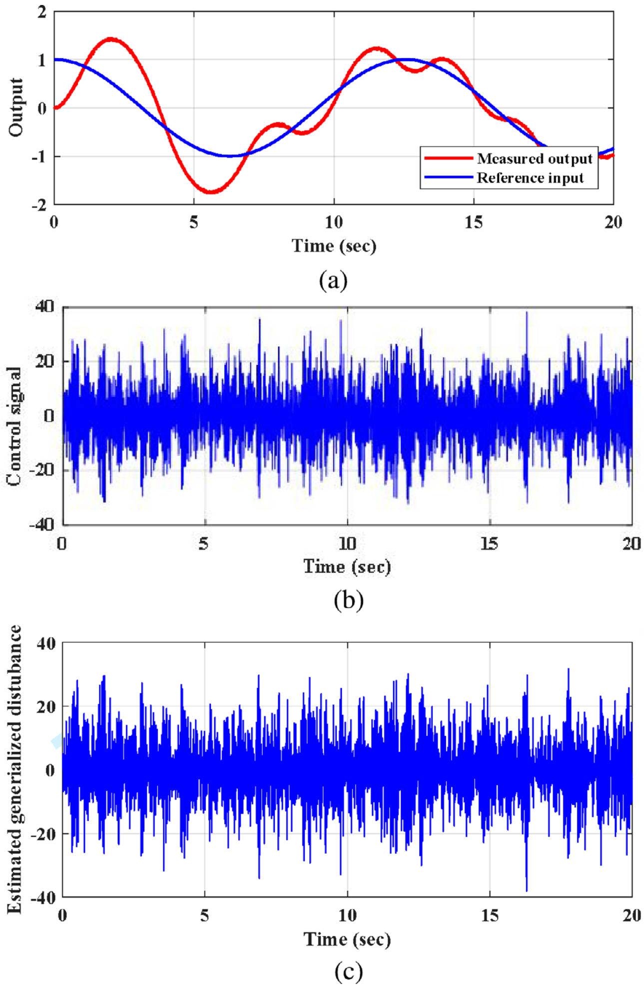

FIGURE 7 Response curves for Case Study 2, (a) tracking y of r, (b) control action u, (c) estimated generalized disturbance $\hat{\xi}_3$.

where r_1 is the desired trajectory and r_2 is its derivative. The parameter R can be selected accordingly to speed up or slow down the transient profile.

The suggested NHOESO-based ADRC is the result of combining the traditional TD of (37), the fal-based control law of (36), and these three components (NADRC). It is employed to detect the estimated states $\left(\widehat{\xi}_1, \widehat{\xi}_2\right)^T$ and the estimated generalized disturbance $\widehat{\xi}_3$, see Figure 5.

To assess the behaviour of the proposed NHOESO, four simulation case studies involving the measurement noise are considered in this section. These scenarios are:

Case Study 1. The LESO is tuned for the smallest integral time absolute error (ITAE) and integral of square energy (ISE) with no noise and simulated with measurement noise, where ITAE $= \int_0^{t_f} t|e|\,dt$ and ISE $= \int_0^{t_f} v^2\,dt$. The ITAE is a measure used in control system engineering to evaluate how well a controlled variable tracks a desired setpoint over time. It considers the magnitude and duration of the error between the setpoint and the actual response. The ITAE criterion combines the absolute error and time by taking their integral. It penalizes both steady-state errors and oscillations in the system response. Minimizing the ITAE is a common goal in control system design to achieve accurate and responsive control. Whereas, integral of square error (ISE) is a metric used in control systems to assess performance. It quantifies the integral of the squared difference between the desired output and the actual output over a specific period. The ISE is calculated by integrating the squared error values. Its purpose is to minimize cumulative squared errors by adjusting control parameters or system dynamics.

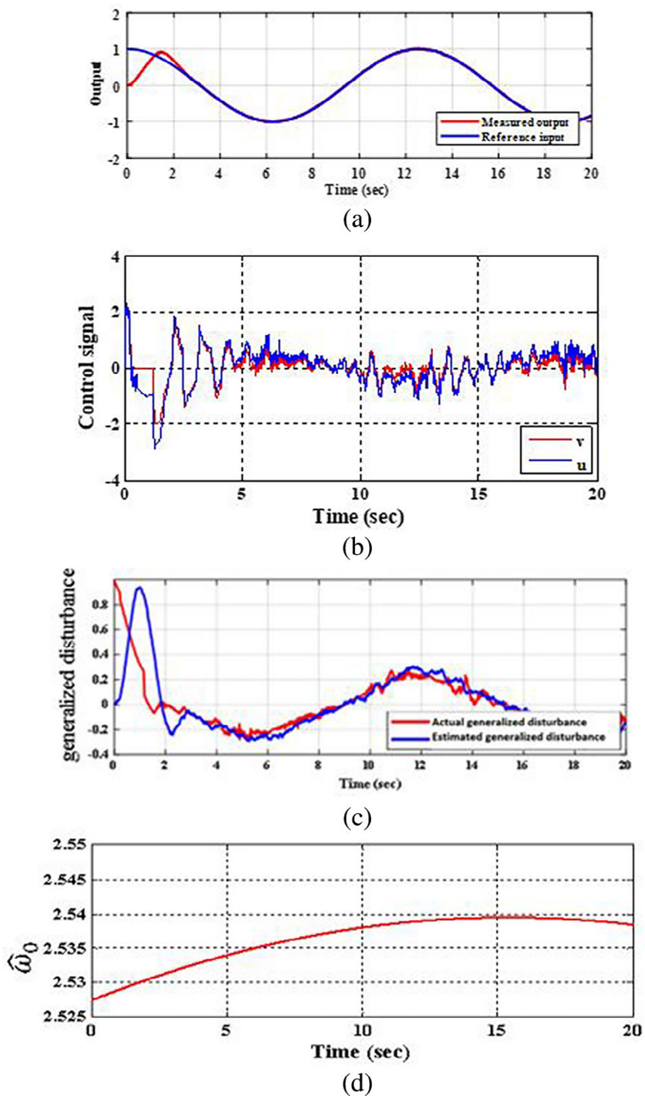

FIGURE 8 Response curves for Case Study 3, (a) tracking y of r, (b) control action u, (c) estimated generalized disturbance $\widehat{\xi}_3$, (d) the time-varying bandwidth $\widehat{\omega}_0$.

Case Study 2. The NHOESO is tuned for the smallest ISE and ITAE with no noise and validated with measurement noise.

Case Study 3. Validating the NHOESO observer in the presence of noise using the time-varying bandwidth TVB technique.

Case Study 4. Testing the NHOESO observer in the presence of noise using the OARU technique.

The time domain response of these four situations is depicted in Figures 6–10 respectively.

Figure 6a depicts the most unfavourable tracking, where the LESO showed bad behaviour versus noise with an ITAE of 41.347519. To lessen the noise effect, numerous alternatives have been conducted. Alter the migratory routes that noise takes to reach those exposed, we can reduce and prevent noise pollution by avoiding extremely noisy recreational activities, choosing alternate forms of transportation over driving a car, doing our chores at recommended times, insulating our homes with noise-absorbing materials, and more. Firstly, the NHOESO has been optimized in a noiseless environment. Subsequently, the NHOESO with its tuned coefficients is validated in a noisy environment. An average assessment of the volume of sound an acoustic product can absorb is called a noise reduction coefficient.

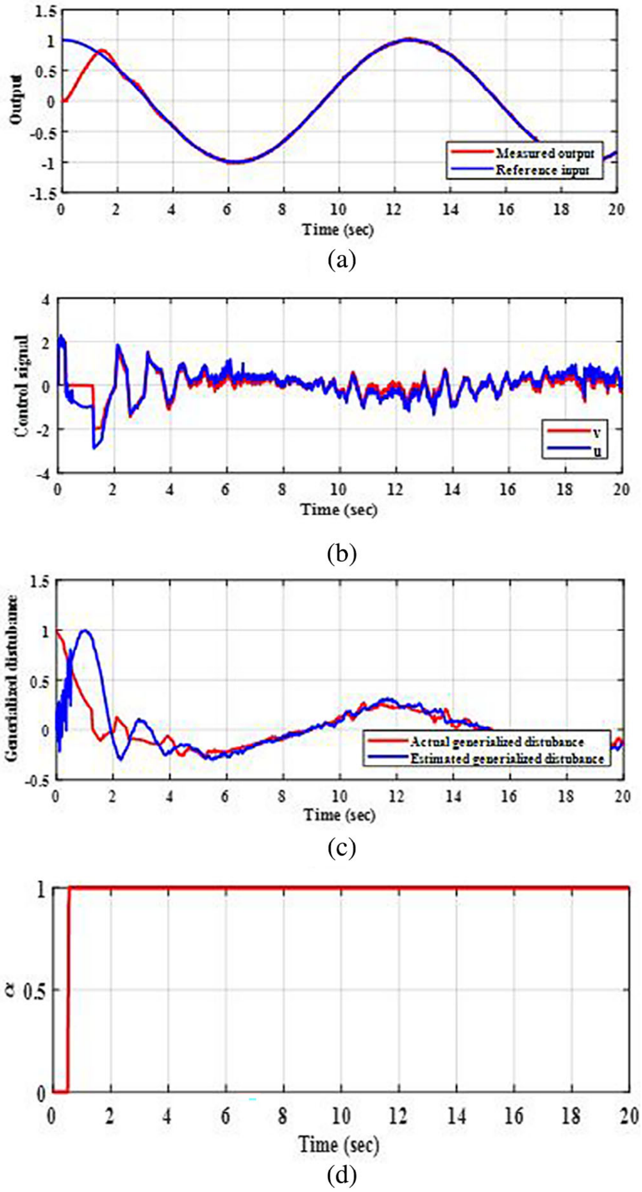

FIGURE 9 Response curves for Case Study 4, (a) tracking y of r, (b) control action u, (c) estimated generalized disturbance $\hat{\xi}_3$, (d) the curve of the adaptive α.

Figure 7 illustrated an improved response for the tracking with an ITAE of 1.321808 and an immense reduction in the estimated generalized disturbance and the control signal chattering with an ISE of 28.825156.

It can be noticed from Figures 8 and 9 that both time responses are similar to each other and the control signal for the case using the ORAU technique is much smoother than that of the TVB technique. One whose controller output depends upon both the instant of viewing as well as the period of transmission of the original signal is said to have a time-variant system. Whereas a secondary microphone picks up sound that is unrelated to the information-bearing transmission but connected to the disturbance picked up by the main sensor, a main microphone still records the chaotic incoming signal.

Figure 10 showed the estimated states of the system given in (16) using the four case studies discussed. The estimated states of the third and fourth case studies are the smoothest in comparison to the first two case studies. Finally, Table 1 lists the numerical results of the four considerations in terms of both ISE and ITAE. A digital calculation carried out under a script that implements a mathematical model for a physical system is known as a numerical simulation. The boundary element method, finite element method, finite difference method, and discrete element method are some of the numerical techniques utilized in modelling geomaterials.

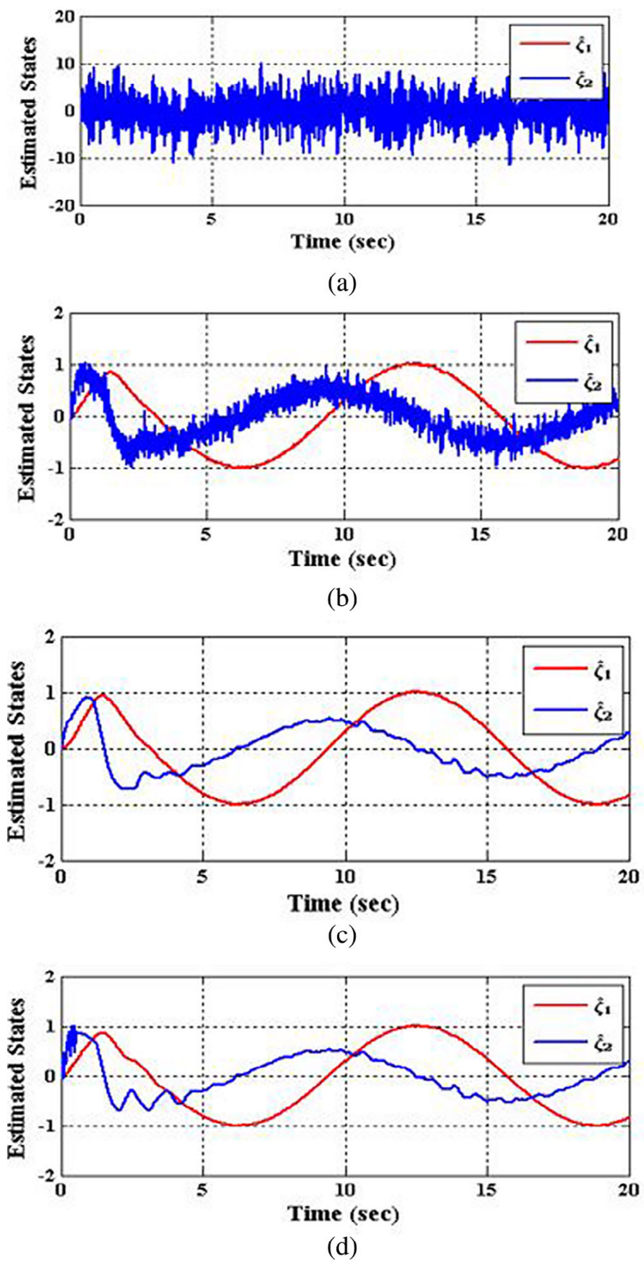

FIGURE 10 The estimated states $\left(\hat{\xi}_1, \hat{\xi}_2\right)^T$ of the four case studies, (a) Case Study 1, (b) Case Study 2, (c) Case Study 3, (d) Case Study 4.

TABLE 1 Performance indices values.

Scenario	ITAE	ISE
1	41.347519	2782.555268
2	1.321808	28.825156
3	1.293564	8.239813
4	1.238883	9.523133

Abbreviations: ISE, integral of square energy; ITAE, integral time absolute error.

It is clear from Table 1 that the large values of ITAE and ISE indicate that measurement noise has a significant impact on the LESO, resulting in a significant decrease in the performance indices for scenario 2 in comparison with scenario 1.

7 | DISCUSSION

In this work, two adaptive NHOESO-based schemes are proposed for countering the measurement noise $\mathcal{N}$. The TVB scheme is the simplest adaptive noise cancellation technique that defines the range and the domain of the bandwidth in the time domain by using three tuneable parameters. A parameter that can be altered by the user while the simulation is running is known as a tuneable parameter. For each dialogue parameter that the macro uses, indicate its tunability using the macro ssSetSFcnParamTunable in mdlInitializeSizes. Remarkably, dialogue parameters can be changed by default. The cut-off frequency of an ideal brick wall filter with noise power roughly equal to the noise power of the original filter is the effective noise bandwidth of any component or system. Hence, performance suffers as a result of noise as a stressor. Both introverts and extroverts have slower reaction times in noisy environments. The main limitation of this technique is that the bandwidth time-varying $\widehat{\omega}_0$ is a function of three predetermined parameters, which leads to the fixed shape of NHOESO's bandwidth. For noise frequencies that occur in the same range where the NHOESO bandwidth is high, the noise $\mathcal{N}$ will be amplified due to large values of the gain parameters $a_i.\widehat{\omega}_0^i, i \in \{1,2,\ldots,\rho+2\}$ in the error-correcting term $\left(a_i.\widehat{\omega}_0^i g\left(y-\widehat{\xi}_i\right)\right)$ of the NHOESO, where $\widehat{\omega}_0$ is a TVB. This results in the NHOESO producing a high chattering in its output estimations $\left(\widehat{\xi}_1,\widehat{\xi}_2,\ldots,\widehat{\xi}_{\rho+1}\right)^T$. Another challenge with this technique is the correct choice of the centre time t_c. In the simulations presented in this work, the value of t_c was found as a result of an optimization process for the nonlinear system of (16). Practically, the selection of this parameter is application dependent and must be done with care because an incorrect choice of t_c value leads to noise being passed into the system through the NHOESO. Therefore, a smart adaptive technique that depends on the existence of noise to switch an online procedure for attenuating the noise is developed, namely, the OARU technique. The sophisticated OARU-NHOESO is the best choice in terms of increasing or reducing the bandwidth as needed, based on the presence of noise. This leads to two main sets of NHOESO parameters: a set of parameters for the measurement of noise Λ_u, and the second set of parameters for the noise-free case Λ_l.

The major limitations and challenges of the proposed techniques are discussed as follows: The technique's primary constraint is that the bandwidth, which is a function of three pre-determined parameters, has a time-varying angular frequency denoted as $\widehat{\omega}_0$. As a result, the shape of NHOESO's bandwidth remains constant. Also, the time required to sense the presence of noise and switch between the parameter sets is higher.

8 | CONCLUSIONS

The use of sensors is vital in control systems for providing the controller with necessary information about the operating environment. These sensors are responsible for most of the measurement noise, which adversely affects controller performance and accuracy. The ESO is the core unit of the active disturbance rejection control, which is extremely influenced by the measurement noise. The two adaptive techniques proposed to address this issue, namely the TVB and OARU, are successful design tools for alleviating the negative effects of measurement noise. The TVB is simpler than OARU as only a single adaptive parameter is needed to account for the measurement noise, that is, the observer bandwidth. The OARU technique proves to be smarter than the TVB as it can sense the presence of the noise components in the output and acts upon this. As such, the conclusion drawn from this is that the OARU is slower than the TVB technique and bears more complexity for tuning several parameters to adaptively account for the measurement noise.

CONFLICT OF INTEREST STATEMENT

The authors declare no conflicts of interest.

DATA AVAILABILITY STATEMENT

Data sharing is not applicable to this article as no new data were created or analyzed in this study.

ORCID

Ibraheem K. Ibraheem https://orcid.org/0009-0003-0819-8912

REFERENCES

Abdul-Adheem, W. R., Azar, A. T., Ibraheem, I. K., & Humaidi, A. J. (2020). Novel active disturbance rejection control based on nested linear extended state observers. *Applied Sciences*, *10*(12), 4069.

Abdul-Adheem, W. R., Ibraheem, I. K., Humaidi, A. J., & Azar, A. T. (2021). Model-free active input–output feedback linearization of a single-link flexible joint manipulator: An improved active disturbance rejection control approach. *Measurement and Control*, *54*(5–6), 856–871.

Alain, K. S. T., Azar, A. T., Bertrand, F. H., & Romanic, K. (2019). Robust observer-based synchronisation of chaotic oscillators with structural perturbations and input nonlinearity. *International Journal of Automation and Control*, *13*(4), 387–412.

Ali, D., Asim, M., Wallam, F., Abbas, A., & Naudhani, Y. (2019, January). Experimental testing of observers comprising discrete Kalman filter and high-gain observers. In *Second International Conference on Computing, Mathematics and Engineering Technologies (iCoMET)* (pp. 1–5). IEEE.

Azar, A. T., & Serrano, F. E. (2018). Adaptive decentralised sliding mode controller and observer for asynchronous nonlinear large-scale systems with backlash. *International Journal of Modelling, Identification and Control*, *30*(1), 61–71.

Azar, A. T., Serrano, F. E., Rossell, J. M., Vaidyanathan, S., & Zhu, Q. (2020). Adaptive self-recurrent wavelet neural network and sliding mode controller/observer for a slider crank mechanism. *International Journal of Computer Applications in Technology*, *63*(4), 273–285.

Chen, B., Huang, Z., Liu, W., Zhang, R., Zhou, F., & Peng, J. (2019, October). A novel adhesion force estimation for railway vehicles using an extended state observer. In *IECON 2019-45th Annual Conference of the IEEE Industrial Electronics Society* (Vol. 1, pp. 225–230). IEEE.

Chen, Z., & Xu, D. (2016). Output regulation and active disturbance rejection control: Unified formulation and comparison. *Asian Journal of Control*, *18*(5), 1668–1678.

Ding, K., & Zhu, Q. (2021). Extended dissipative anti-disturbance control for delayed switched singular semi-Markovian jump systems with multi-disturbance via disturbance observer. *Automatica*, *128*, 109556.

Djeddi, A., Dib, D., Azar, A. T., & Abdelmalek, S. (2019). Fractional order unknown inputs fuzzy observer for Takagi–Sugeno systems with unmeasurable premise variables. *Mathematics*, *7*(10), 984.

Du, H., Qian, C., Frye, M. T., & Li, S. (2012). Global finite-time stabilisation using bounded feedback for a class of non-linear systems. *IET Control Theory & Applications*, *6*(14), 2326–2336.

Guo, B. Z., & Wu, Z. H. (2017). Output tracking for a class of nonlinear systems with mismatched uncertainties by active disturbance rejection control. *Systems & Control Letters*, *100*, 21–31.

Han, J. (2009). From PID to active disturbance rejection control. *IEEE Transactions on Industrial Electronics*, *56*(3), 900–906.

Huang, S. C., Nguyen, Q. D., & Su, T. J. (2020). Disturbance observer-based linear matrix inequality for the synchronization of Takagi-Sugeno fuzzy chaotic systems. *IEEE Access*, *8*, 225805–225821.

Kammogne, A. S. T., Kountchou, M. N., Kengne, R., Azar, A. T., Fotsin, H. B., & Ouagni, S. T. M. (2020). Polynomial robust observer implementation based passive synchronization of nonlinear fractional-order systems with structural disturbances. *Frontiers of Information Technology & Electronic Engineering*, *21*, 1369–1386.

Łakomy, K., & Madonski, R. (2021). Cascade extended state observer for active disturbance rejection control applications under measurement noise. *ISA Transactions*, *109*, 1–10.

Li, X., & Xia, H. (2020). A new extended state observer with low sensitivity to high-frequency noise and low gain power. *IFAC-PapersOnLine*, *53*(2), 4929–4934.

Liaquat, M., Javaid, M. A., & Saad, M. (2017, October). A nonlinear high-gain observer for an n-link robot manipulator which has measurement noise in a feedback control framework. In *17th International Conference on Control, Automation and Systems (ICCAS)* (pp. 755–759). IEEE.

Linares, E., Amador, M., Hernández-Cortés, T., López-Estrada, F. R., & Estrada-Manzo, V. (2022, November). Actuator and sensor fault estimation of the Furuta pendulum system via linear matrix inequalities. In *XXIV Robotics Mexican Congress (COMRob)* (pp. 84–88). IEEE.

Madoński, R., & Herman, P. (2012, November). Method of sensor noise attenuation in high-gain observers—Experimental verification on two laboratory systems. In *IEEE International Symposium on Robotic and Sensors Environments Proceedings* (pp. 121–126). IEEE.

Meyer, L., Ichalal, D., Vigneron, V., & Vasiljevic, C. (2017, October). Minimum variance unbiased observer of a continuous LPV system with unknown input. In *IEEE International Conference on Systems, Man, and Cybernetics (SMC)* (pp. 2603–2607). IEEE.

Mu, Y., Zhang, H., Yan, Y., & Wu, Z. (2022). A design framework of nonlinear H∞ PD observer for one-sided Lipschitz singular systems with disturbances. *IEEE Transactions on Circuits and Systems II: Express Briefs*, *69*(7), 3304–3308.

Przybyła, M., Kordasz, M., Madoński, R., Herman, P., & Sauer, P. (2012). Active disturbance rejection control of a 2DOF manipulator with significant modelling uncertainty. In *Bulletin of the Polish Academy of Sciences: Technical Sciences* (pp. 509–520). Polish Academy of Sciences.

Pu, Z., Yuan, R., Yi, J., & Tan, X. (2015). A class of adaptive extended state observers for nonlinear disturbed systems. *IEEE Transactions on Industrial Electronics*, *62*(9), 5858–5869.

Sun, J., Wang, C., & Xin, R. (2018, July). On disturbance rejection control of servo system based on the improved disturbance observer. In *37th Chinese Control Conference (CCC)* (pp. 2554–2559). IEEE.

Tamhane, B., Kurode, S., & Bandyopadhyay, B. (2018, July). Novel higher-order sliding mode observer for output noise attenuation. In *15th International Workshop on Variable Structure Systems (VSS)* (pp. 297–302). IEEE.

Vargas, J. A. R., & Hemerly, E. M. (2000, December). Nonlinear adaptive observer design for uncertain dynamical systems. In *Proceedings of the 39th IEEE Conference on Decision and Control* (Cat. No. 00CH37187) (Vol. 2, pp. 1307–1308). IEEE.

Xue, W., & Huang, Y. (2014). On performance analysis of ADRC for a class of MIMO lower-triangular nonlinear uncertain systems. *ISA Transactions*, *53*(4), 955–962.

Yamada, Y., Nozaki, T., & Murakami, T. (2019, October). Observer structure considering reluctance torque of IPMSM for noise resistance. In *IECON 2019-45th Annual Conference of the IEEE Industrial Electronics Society* (Vol. 1, pp. 461–466). IEEE.

Yang, J., & Ding, Z. (2017). Global output regulation for a class of lower triangular nonlinear systems: A feedback domination approach. *Automatica*, *76*, 65–69.

Zhu, Q. (2018). Stabilization of stochastic nonlinear delay systems with exogenous disturbances and the event-triggered feedback control. *IEEE Transactions on Automatic Control*, *64*(9), 3764–3771.

AUTHOR BIOGRAPHIES

Ahmed Alkhayyat (Member, IEEE) received the BSc degree in electrical engineering from AlKufa University, Najaf, Iraq, in 2007, the M.Sc. degree from the Dehradun Institute of Technology, Dehradun, India, in 2010, and the PhD degree from Cankaya University, Ankara, Turkey, in 2015. He is currently the Dean of International Relationship and a Manager of the word ranking with Islamic University, Najaf. His research interests include the IoT in the health-care systems, SDN, network coding, cognitive radio, efficient-energy routing algorithms, and efficient-energy MAC protocol in cooperative wireless networks and wireless body area networks, as well as cross-layer designing for self- organized networks. He contributed in organizing a several IEEE conferences, workshop, and special sessions. To serve his community, he acted as a reviewer for several journals and conferences.

Ali Mahdi Zalzala received his BSc and MSc in Electrical Engineering from the University of Baghdad, College of Engineering on 1982 and 1986, respectively. He received his PhD in Wireless and mobile systems from USM, Malaysia on 2016. He worked as a lecturer at University of Baghdad and Ibb University-Yemen and worked in industry for more than 20 years on development of industrial and RF systems. He is currently head of department of Electronics and Communication Engineering at Uruk University, Iraq. His interests include electronic and embedded systems and wireless communication systems.

Dr. Asaad A. M. Al-Salih, 68 years old, Iraqi national, 35 years of service (BSc Elec. Eng., MSc Elec. Eng., PhD Systems Eng., Member IEEE, Consultant Electrical & Computer Engineer) is an Associate Professor in the Dept. Elec. Eng., College of Eng., University of Baghdad (Iraq) since December 2002. Earlier, he was an Assistant Professor in the same department from June 1998 to November 2002, and a Lecturer in the said department from July 1985 to May 1998. For the period December 1986 to September 1990 he has been involved in teaching and research work activities in the Department of Computation, Manchester University (UK). He has been selected in March 2004 as a recipient by the Iraqi Government to get a PhD in Systems Engineering of Image Processing through a scholarship given by the GCSS Scheme of the Indian Council for Cultural Relations (ICCR). For the period May 2005 to May 2010, he was doing his PhD in the field of Image Processing & Computer Vision in the Department of Computer Science at Jamia Millia Islamia University – New Delhi, where he sets up an "Embedded Systems & Image Processing" research lab in the said department. Al-Salih has held a number of engineering research and teaching positions in Iraq. This involved teaching in the B.Sc. course, advanced M. Sc. courses, and supervising research theses in Electrical & Computer Engineering topics. He was, meanwhile, senior member of the Computer Technology Research Group, Coordinator of the Image Processing & Computer Vision Applications Program, and a co-senior faculty-in-charge of the Curriculum Development Group. For the 3 successive academic years 1999/2000, 2000/2001, and 2001/2002 he received the Iraqi State Award for the Outstanding Scientific Faculty Member. He, besides, received in the year 2000, the State Felicitation of the Iraqi Day of Science. His fields of interest are: image processing, computer vision, machine vision, robotic vision, IT, systems analysis and design, metamaterial electronics, and acoustics. Al-Salih has supervised and reviewed several M.Sc. and Ph.D. theses. He has so far published 45 publications including 12 journal papers (3 by Elsevier), 10 separate books-chapters published by Macmillan and Springer, 6 papers in IEEE international conferences (2 of which in IEEE Computer Society), 9 in specialized international conferences, 4 in national conferences, 2 theses, and 2 technical reports.

Prof. Dr. Anwar Ja'afar Mohamed Jawad was born in Baghdad, Iraq (1961). He is one of the academic staff in Al-Rafidain University College, Baghdad-Iraq. His designation is professor in Applied Mathematics from (2014). The academic Qualifications are PhD in Applied Mathematics from University of Technology, Baghdad, (2000), MSc in Operation Research from University of Technology, Baghdad, (1989), and BSc in Mechanical Engineering from Baghdad University, (1983). He is interested in Differential equations, and Numerical analysis. He published in Scopus and Clarivate journals more than 95 papers in Mathematics, Soliton, and Solving Nonlinear Partial Differential Equations NLPDEs. He was teaching Mathematics, numerical analysis for graduate and postgraduate students in Iraqi and Syrian universities. He was a supervised for many MSc. and PhD. Thesis.

Wameedh Riyadh Abdul-Adheem received the BS degree (with highest honors) in electrical engineering in 1998, the MS degree in computer and control engineering in 2001, and PhD degree in computer and control engineering in 2019 all from the University of Baghdad at Baghdad. His research interests include signal processing, nonlinear control, and optimization.

Jamshed Iqbal (Senior Member, IEEE) received the PhD degree in robotics from the Italian Institute of Technology (IIT) and the three master's degrees in various fields of engineering from Finland, Sweden, and Pakistan. He is currently working as a Research Associate Professor with the University of Jeddah, Saudi Arabia. With more than 20 years of multi-disciplinary experience in industry and academia, his research interests include robot analysis, and design and control. He has more than 60 journal articles on his credit with H-index of 26.

Ibraheem K. Ibraheem was born in Baghdad, Iraq, in 1976. He received the BS degree in electrical engineering from the University of Baghdad, Baghdad, Iraq in 1998 and MSc & PhD. degrees in Computer & Control Engineering from the same university and department, in 2001 and 2007, respectively. In 2015 he visited High-Performance Computing Lab. in Ashburn/Virginia at George Washington University/USA for a cooperative research on the hardware implementation of nonlinear control. In 2019 he became a Professor of electrical engineering at the electrical engineering department/Baghdad University. His research interests include active disturbance rejection control, power control, Robotics, signal processing, nonlinear control and intelligent control applications.

Waleed K. Ibraheem is an Instructor at the Department of Medical Instruments Engineering Techniques, Al-Farahidi University College. Hi is field of interests includes optimization, Networking, and mathematics.

Mustafa Musa Jaber received the PhD degree from University Tun Hussein Onn Malaysia. He is currently pursuing the PhD degree with the Technical University of Malaysia. His research interests include telemedicine, machine learning, and human factor.

Asaad Shakir Hameed is an instructor at the University of Mazaya, Department of Quality Assurance.

How to cite this article: Alkhayyat, A., Zalzala, A. M., AL-Salih, A. A. M., Jawad, A. J. M., Abdul-Adheem, W. R., Iqbal, J., Ibraheem, I. K., Ibrahim, W. K., Jaber, M. M., & Hameed, A. S. (2023). A novel class of adaptive observers for dynamic nonlinear uncertain systems. *Expert Systems*, e13412. https://doi.org/10.1111/exsy.13412